

Electronic supplementary information (ESI) for

**Monitoring hydrogen transport through graphene by in situ surface-enhanced Raman spectroscopy**

Younghyun Wy,<sup>‡a</sup> Jaesung Park,<sup>‡b</sup> Sung Huh,<sup>a</sup> Hyuksang Kwon,<sup>b</sup> Bon Seung Goo,<sup>a</sup> Jung Young Jung,<sup>a</sup> and Sang Woo Han<sup>\*a</sup>

<sup>a</sup>*Center for Nanotectonics, Department of Chemistry and KI for the NanoCentury, KAIST, Daejeon 34141, Korea. E-mail: sangwoohan@kaist.ac.kr*

<sup>b</sup>*Korea Research Institute of Standards and Science (KRISS), Daejeon 34113, Korea*

<sup>‡</sup>These authors contributed equally to this work.

**Contents**

1. Experimental details
2. Supplementary figures: Fig. S1-S6

## 1. Experimental details

**Chemicals and materials.** Graphite flakes (NGS Naturgraphit GmbH), PMMA solution ( $M_w = 495,000$ , 5% in anisole, Kayaku Advanced Materials), poly(4-styrenesulfonic acid) (PSS) solution ( $M_w = 75,000$ , 18 wt% in  $H_2O$ , Sigma-Aldrich), silver nitrate (Sigma-Aldrich), poly(vinylpyrrolidone) (PVP,  $M_w = 55,000$ , Sigma-Aldrich), trisodium citrate dihydrate (Aldrich), potassium iodide (Sigma-Aldrich), hydrogen tetrachloroaurate(III) trihydrate (Sigma-Aldrich),  $NaBH_4$  (Sigma-Aldrich), ethanol (Daejung Chemicals & Metals Co.), hydrogen peroxide (Daejung Chemicals & Metals Co.), ascorbic acid (Daejung Chemicals & Metals Co.), and 4-NTP (TCI) were used as received. Deionized water with a resistivity of greater than  $18.0\text{ M}\Omega\cdot\text{cm}$  was used in the preparation of aqueous solutions.

**Synthesis of Au NPCs.** Au NPCs consisting of NPs with an average size of 30 nm were prepared based on our previous report.<sup>S1</sup> As a sacrificial template, Ag nanoprisms were prepared first. 0.6 mL of an aqueous silver nitrate solution (5 mM) and 25.5 mL of deionized water were mixed in a 100 mL Erlenmeyer flask with vigorous stirring at room temperature. 1.8 mL of an aqueous sodium citrate solution (30 mM) and 1.8 mL of an aqueous PVP solution ( $5\text{ mg mL}^{-1}$ ) were added to this solution. After 3 min, 60  $\mu\text{L}$  of hydrogen peroxide and 300  $\mu\text{L}$  of an aqueous  $NaBH_4$  solution (100 mM) were added to the reaction solution. Ag nanoprisms were formed after 30 min. To prepare Au NPCs, 20 mL of an aqueous PVP solution ( $10\text{ mg mL}^{-1}$ ), 10 mL of an aqueous sodium citrate solution (60 mM), and 10 mL of deionized water were mixed in a 100 mL Erlenmeyer flask with vigorous stirring at room temperature. To this solution, 5 mL of an aqueous hydrogen tetrachloroaurate(III) solution (10 mM), 0.6 mL of an aqueous potassium iodide solution (50 mM), and 0.9 mL of an aqueous ascorbic acid solution were added sequentially. After 30 s, 2 mL of the Ag nanoprism solution was added to the reaction solution. Au NPCs were collected and washed 3 times with ethanol by centrifugation (4000 rpm for 5 min). The prepared Au NPCs were dispersed in 200  $\mu\text{L}$  of ethanol for future use.

**Device fabrication.** To fabricate the pattern of Au NPCs on a substrate, PMMA was spin-coated on a Si substrate with a 300 nm of silica layer and patterned by electron-beam lithography to form an array of square-shaped holes. 2  $\mu\text{L}$  of a concentrated Au NPCs solution was dropped and spin-coated 10 times at 3000 rpm on the PMMA-patterned Si wafer. The wafer coated with Au NPCs was washed with acetone for the lift-off process and immersed in a  $10^{-4}\text{ M}$  ethanol solution of 4-NTP for 2 h, and then thoroughly washed with ethanol. To deposit defect-free monolayer graphene on the patterned Au NPCs, we applied a dry transfer technique, which is a well-known method for the fabrication of the multifunctional high-performance van der Waals heterostructures.<sup>S2,S3</sup> We confirmed the presence of monolayer graphene on the PMMA-coated substrate with optical microscopy and Raman spectroscopy. After the transfer of monolayer graphene on the Au NPCs, electron-beam lithography, electron-beam evaporator, and reactive ion etcher were utilized to make a metal mask, Au/Ti, with a thickness of 20 nm/2 nm and a width of 3  $\mu\text{m}$ . The thicknesses of Au and Ti were monitored by a quartz crystal microbalance in the electron-beam evaporator.

**Characterizations.** A FEI-Tecnai G2 F30 Super-Twin transmission electron microscope operated at 300 kV and a FEI-INSPECT F50 field-emission scanning electron microscope were used to characterize Au NPCs. An optical microscope (Leica DM2700M) with an objective lens ( $\times 100$ , NA = 0.9) was used to observe samples. A scanning probe microscope (XE-100) was used to get the surface morphology of samples. Raman spectra were obtained with a Raman microscope equipped with an integral microscope (Olympus BX 43), spectrometer (Acton Spectra Pro 2300i), and a thermoelectrically cooled charge-coupled device detector (ANDOR, DV401A-BV,  $1024 \times 127$  pixels). The 633 nm line of an air-cooled He/Ne laser and the 532 nm line of a continuous-wave diode-pumped laser were used as excitation sources. The laser beam was focused on a device with an objective lens ( $\times 50$ , NA = 0.55). A holographic grating ( $1200$  grooves  $\text{mm}^{-1}$ ) and a slit allowed the spectral resolution to be  $1$   $\text{cm}^{-1}$ . Raman mapping images were obtained with a WITec alpha300R Raman imaging microscope. The 532 nm line of a diode-pumped solid-state laser with a power of 1 mW was used for the Raman mapping of graphene on a device. The 633 nm line of a He/Ne laser with a power of 10  $\mu\text{W}$  was used for the Raman mapping of 4-NTP on a device. The laser beam was focused on a sample with an objective lens ( $\times 100$ , NA = 0.9). Raman mapping images were collected with a step size of 0.25  $\mu\text{m}$  and an acquisition time of 1 s for each point. For in situ SERS measurements, an aqueous  $\text{NaBH}_4$  solution (10 mM, 0.2 mL) was dropped onto a device lying on a temperature-controllable stage, and then Raman spectra were obtained every 10 s using a 0.8 mW 633 nm laser with an acquisition time of 1 s.

**The number of adsorbed 4-NTP molecules.** A  $5 \mu\text{m} \times 5 \mu\text{m}$  Au NPCs pattern consists of three layers of close-packed Au nanoparticles with an average size of 30 nm, which was confirmed by atomic force microscopy measurements. Accordingly, the total Au surface area of an Au NPCs pattern could be assumed to be  $\sim 272 \mu\text{m}^2$ . Given that the packing density of 4-NTP molecules on Au is almost identical to that of benzenethiol ( $6.8 \times 10^{14}$  molecules  $\text{cm}^{-2}$ ),<sup>S4</sup> the number of adsorbed 4-NTP molecules can be estimated to be  $\sim 1.8 \times 10^9$ . Since 0.2 mL of 10 mM  $\text{NaBH}_4$  solution was used for the reduction reaction,  $\text{NaBH}_4$  is  $\sim 10^6$  times more abundant than 4-NTP molecules.

**Computational methods.** DFT calculations were performed with the Quantum Espresso package with the Perdew-Burke-Ernzerhof (PBE) exchange-correlation functional.<sup>S5-S7</sup> Grimme's D2 van der Waals correction method was employed together.<sup>S8</sup> Ultrasoft pseudopotentials were utilized to describe the electron-ion attractive interaction terms. To model the graphene surface, 72 carbon atoms were arrayed to form 6-membered hexagonal rings with a C–C bond length of 1.42 Å. The unit cell was designed to possess periodicity along the x- and y-axes and vacuum with a thickness of 30 Å along the z-axis. The  $\text{BH}_4^-$  species on graphene was described as a  $\text{BH}_3$  unit bound to the on-top site of a single carbon and an H bound to the on-top site of the very adjacent carbon. To analyze charged species in the calculation model, its geometry was optimized, followed by self-consistent field calculation. From the result, the Löwdin charge was extracted and analyzed. The  $3 \times 3 \times 1$  and  $7 \times 7 \times 1$  k-point sampling were used in geometry optimization and self-consistent field calculation, respectively. The cutoff energy and the convergence threshold were set to be 40 and  $10^{-4}$  Ry,

respectively.

## References

- S1 S. Lee, S. Kang, J. Kim, Y. Wy and S. W. Han, *ChemNanoMat*, 2017, **3**, 772-778.
- S2 C. R. Dean, A. F. Young, I. Meric, C. Lee, L. Wang, S. Sorgenfrei, K. Watanabe, T. Taniguchi, P. Kim, K. L. Shepard and J. Hone, *Nat. Nanotechnol.*, 2010, **5**, 722-726.
- S3 A. K. Geim and I. V. Grigorieva, *Nature*, 2013, **499**, 419-425.
- S4 A. D. McFarland, M. A. Young, J. A. Dieringer and R. P. Van Duyne, *J. Phys. Chem. B*, 2005, **109**, 11279-11285.
- S5 P. Giannozzi, S. Baroni, N. Bonini, M. Calandra, R. Car, C. Cavazzoni, D. Ceresoli, G. L. Chiarotti, M. Cococcioni, I. Dabo, A. D. Corso, S. Gironcoli, S. Fabris, G. Fratesi, R. Gebauer, U. Gerstmann, C. Gougoussis, A. Kokalj, M. Lazzeri, L. Martin-Samos, N. Marzari, F. Mauri, R. Mazzarello, S. Paolini, A. Pasquarello, L. Paulatto, C. Sbraccia, S. Scandolo, G. Sclauzero, A. P. Seitsonen, A. Smogunov, P. Umari and R. M. Wentzcovitch, *J. Phys. Condens. Matter*, 2009, **21**, 395502.
- S6 P. Giannozzi, O. Andreussi, T. Brumme, O. Bunau, M. B. Nardelli, M. Calandra, R. Car, C. Cavazzoni, D. Ceresoli, M. Cococcioni, N. Colonna, I. Carnimeo, A. D. Corso, S. Gironcoli, P. Delugas, R. A. DiStasio Jr., A. Ferretti, A. Floris, G. Fratesi, G. Fugallo, R. Gebauer, U. Gerstmann, F. Giustino, T. Gorni, J. Jia, M. Kawamura, H.-Y. Ko, A. Kokalj, E. Küçükbenli, M. Lazzeri, M. Marsili, N. Marzari, F. Mauri, N. L. Nguyen, H.-V. Nguyen, A. Otero-de-la-Roza, L. Paulatto, S. Poncé, D. Rocca, R. Sabatini, B. Santra, M. Schlipf, A. P. Seitsonen, A. Smogunov, I. Timrov, T. Thonhauser, P. Umari, N. Vast, X. Wu and S. Baroni, *J. Phys. Condens. Matter*, 2017, **29**, 465901.
- S7 J. P. Perdew, K. Burke and M. Ernzerhof, *Phys. Rev. Lett.*, 1996, **77**, 3865-3868.
- S8 S. Grimme, *Comput. Chem.*, 2006, **27**, 1787-1799.

## 2. Supplementary figures

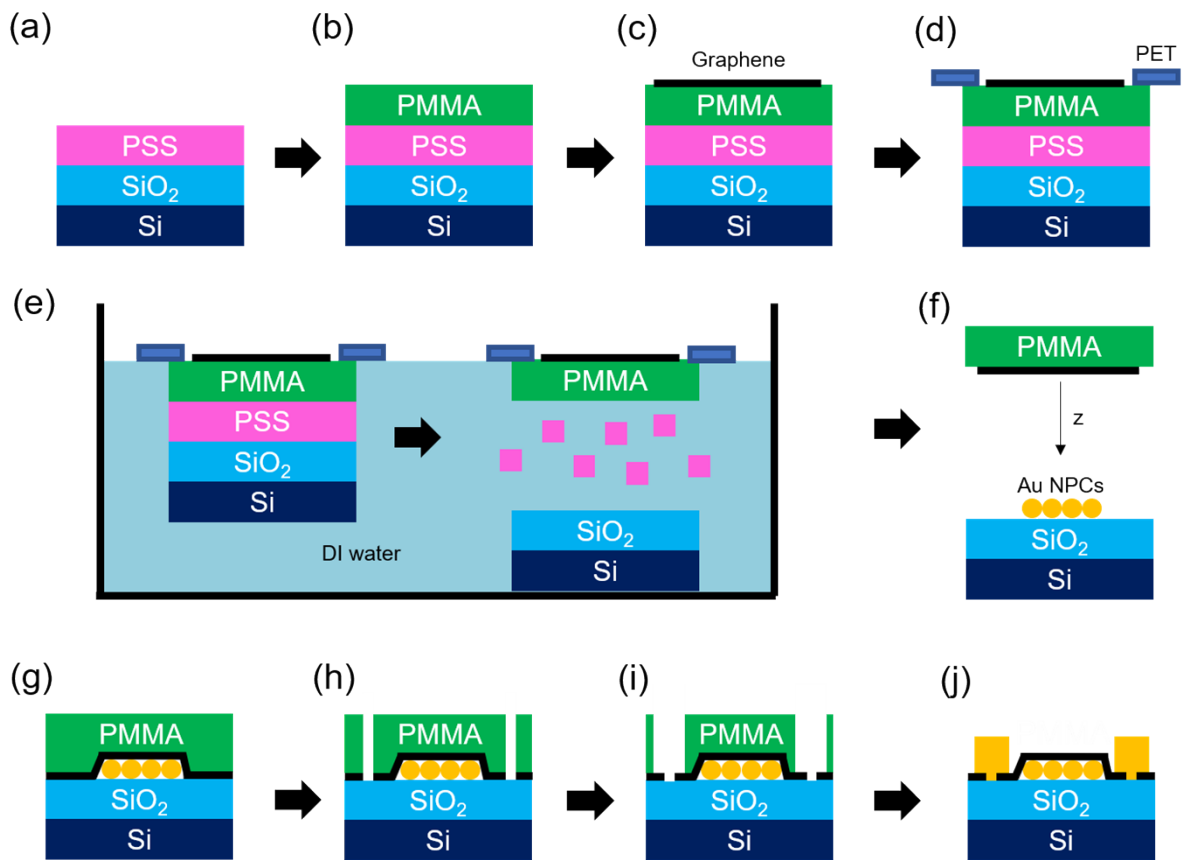


**Fig. S1** Schematic illustration of graphene transfer and metal masking processes. (a,b) PSS and PMMA layers (thickness = 30 nm) were sequentially deposited on a Si wafer with spin coating. (c) Mechanically exfoliated graphene was transferred onto the substrate. (d) A polyethylene (PET) thin film with a hole was tightly fixed on the head side of the substrate with scotch tape. (e) In deionized water, the Si wafer was separated from the upper side by dissolving of PSS layer. (f,g) The graphene supported on PMMA was transferred onto a  $5\ \mu\text{m} \times 5\ \mu\text{m}$  Au NPCs pattern. (h,i) To passivate the boundary of graphene, a selected area of graphene was patterned and etched by electron-beam lithography. (j) An Au/Ti metal mask was deposited using a thermal evaporator.

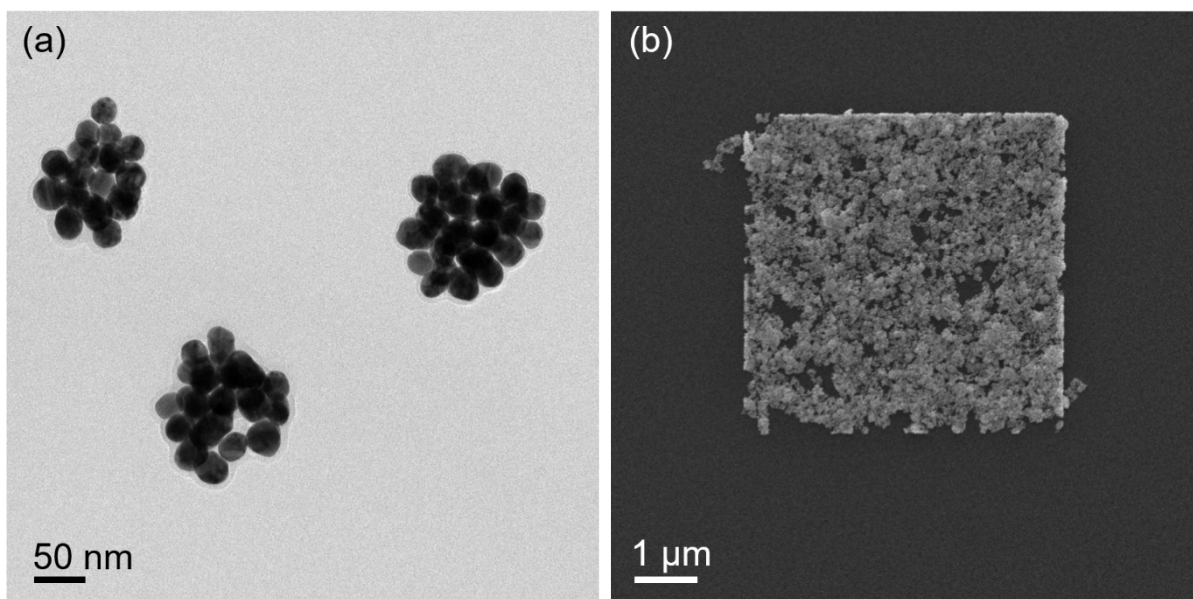


**Fig. S2** (a) Transmission electron microscopy image of Au NPCs. (b) Scanning electron microscopy image of an Au NPCs pattern.

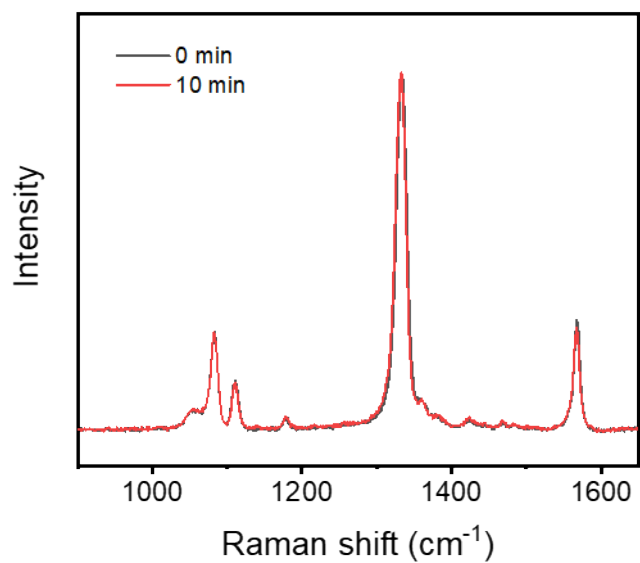


**Fig. S3** SERS spectra obtained at the center of the device before and after the laser irradiation for 10 min without the treatment of NaBH<sub>4</sub>.

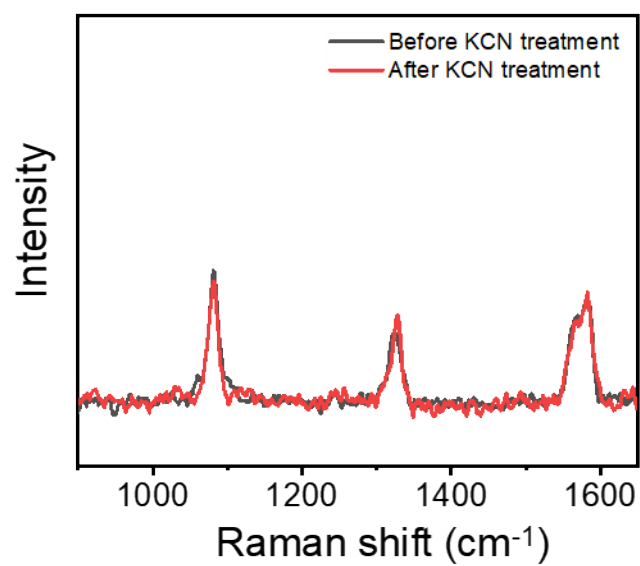


**Fig. S4** SERS spectra obtained at the center of the device before and after KCN treatment.

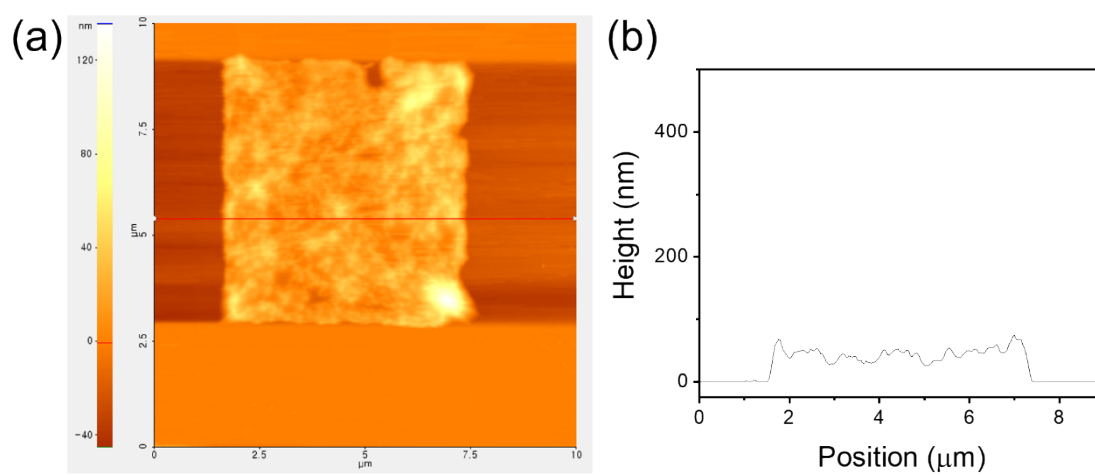


**Fig. S5** (a) Atomic force microscopy image and (b) corresponding height profile of the device before  $\text{NaBH}_4$  treatment.

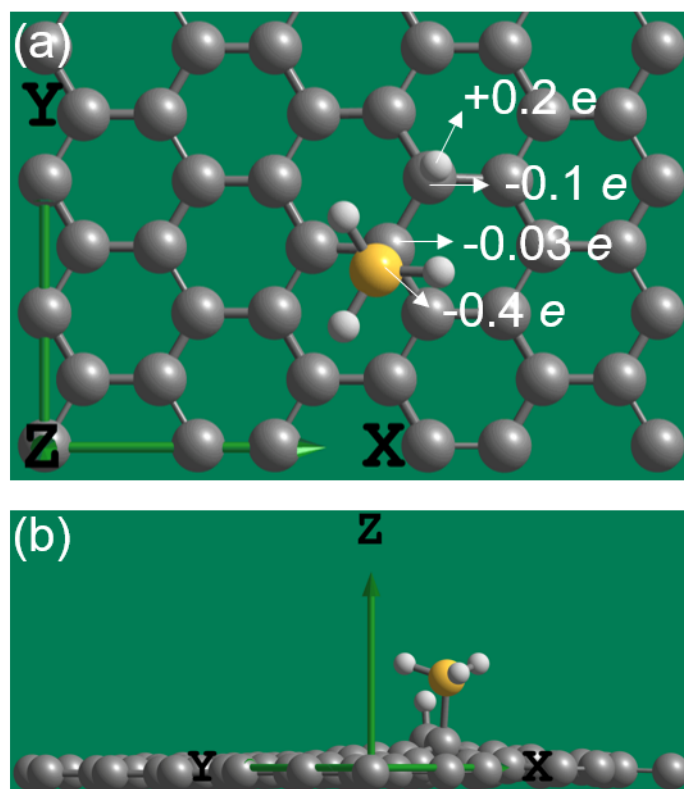


**Fig. S6** (a) Top and (b) side views of DFT-calculated products of the dissociative adsorption of a  $\text{BH}_4^-$  ion on a model graphene surface. Atomic charges obtained through the Löwdin charge analysis are denoted in a.